Photochemical & Photobiological Sciences

Accepted Manuscript

This is an *Accepted Manuscript*, which has been through the Royal Society of Chemistry peer review process and has been accepted for publication.

Accepted Manuscripts are published online shortly after acceptance, before technical editing, formatting and proof reading. Using this free service, authors can make their results available to the community, in citable form, before we publish the edited article. We will replace this *Accepted Manuscript* with the edited and formatted *Advance Article* as soon as it is available.

You can find more information about *Accepted Manuscripts* in the Information for Authors.

Please note that technical editing may introduce minor changes to the text and/or graphics, which may alter content. The journal's standard Terms & Conditions and the Ethical guidelines still apply. In no event shall the Royal Society of Chemistry be held responsible for any errors or omissions in this *Accepted Manuscript* or any consequences arising from the use of any information it contains.

ROYAL SOCIETY OF CHEMISTRY

www.rsc.org/pps

Journal Name

RSCPublishing

ARTICLE

Inverted methoxypyridinium phthalocyanines for PDI of pathogenic bacteria

Leandro M. O. Lourenço,[a] Andreina Sousa,[b] Maria C. Gomes,[a,b] Maria A. F. Faustino,[a] Adelaide Almeida,[b] Artur M. S. Silva,[a] Maria G. P. M. S. Neves,[a] José A. S. Cavaleiro,[a] Ângela Cunha,[b] João P. C. Tomé[a,c*]

Cite this: DOI: 10.1039/x0xx00000x

Received 00th January 2015,
Accepted 00th January 2015

DOI: 10.1039/x0xx00000x

www.rsc.org/

Phthalocyanines (Pc) are photoactive molecules that can absorb and emit light in a large range of the UV-Vis spectrum with recognized potential for medical applications. Considering the biomedical applications an important limitation of these compounds is their low solubility in water. The use of suitable pyridinium groups on Pc is a good strategy to solve this drawback and to make them more effective to photoinactivate Gram-negative bacteria *via* photodynamic inactivation (PDI) approach. In here, it is described an easy synthetic access to obtain inverted tetra- and octa-methoxypyridinium phthalocyanines (compounds **5** and **6**) and also their efficiency to photoinactivate a recombinant bioluminescent strain of *Escherichia coli*. The obtained results were compared with the ones obtained when more conventional thiopyridinium phthalocyanines (compounds **7** and **8**) were used. This innovative study of compared thiopyridinium and inverted methoxypyridinium moieties on cationic Pc is the first time that is provided taking into account the efficiency of singlet oxygen ($^1O_2$) generation, water solubility and uptake properties.

Introduction

Phthalocyanines (Pc),[1,2] and the corresponding analogues, are well-known conjugated aromatic compounds which have been intensively studied in many scientific areas due to their absorption in the red and near-infrared regions of the electromagnetic spectrum (600-800 nm).[3-5] In particular, Pc derivatives have been exploited as photosensitizers (PS) for photodynamic therapy (PDT), evidencing a high potential in cancer treatment,[6-12] in the photodynamic inactivation (PDI) of (multi)resistant microorganisms in infectious diseases[13-18] and/or in contaminated environmental matrices.[19] All these applications are based on cell death induced by reactive oxygen species (ROS), mainly singlet oxygen ($^1O_2$), generated by the combined action of visible light, molecular oxygen and a PS. Since the chemical structure is a key factor in the PS physicochemical properties, different approaches have been used to introduce specific functionalities on the phthalocyanine core in order to obtain adequate features, namely desired levels of hydrophobicity or hydrophilicity. The molecular structure of unsubstituted Pc can be modified through the incorporation of substituents in the peripheral positions of the tetraazaisoindole macrocycle to improve their amphiphilicity,[8] or by metallation with different metal ions (Zn, Si, Al, Ga or In) in the cavity of the Pc core,[20] that can result in an enhancement of the triplet state parameters (triplet quantum yield and lifetime) and $^1O_2$ quantum yield.[21,22] The addition of axial ligands in coordinative positions of such metal centres can also improve the efficiency of these compounds as PS.[23-29] These modifications can unequivocally modulate the photophysical and photochemical characteristics of Pc derivatives and affect their interaction with cells, triggering different photobiological effects.[3,30]
The emergent antibiotic-resistance observed in pathogenic bacteria has prompted the search for new and more efficient therapeutic modalities as it is antibacterial PDI approach.[13,31-33] The ability of Pc to interact with bacteria and their capability to generate ROS have been related with the efficiency of bacterial inactivation mediated by oxidative stress exerted in different cellular targets.[34]
It is well established that in general, the use of photoactive cationic PS is required for an efficient photodynamic inactivation of Gram-negative bacteria.[13,35-39] The positive charged PS derivatives can interact electrostatically with the negative charged components of the outer wall (lipoproteins, lipopolysaccharides) which favours PS binding to Gram-negative bacteria, increasing the efficiency of photodynamic activity.[40] The inactivation of Gram-positive bacteria can be attained with neutral, anionic and cationic PS which promptly cross the relatively porous cell wall.[14,41-44] Considering PDI as a promising methodology for the treatment of microbial infections[13-16,18] or contaminated media,[45] this work aims to establish relations between the chemical structure of innovative inverted methoxypyridinium Pc **5** and **6** (Scheme 1) and their efficiency as PS for the inactivation of microbial strains. The synthesis and structural characterization of these cationic Pc and of the required precursors, phthalonitriles (**1** and **2**) and neutral pyridinones Pc **3** and **4** are also described. The ability of the new water soluble Pc to photoinactivate microorganisms was evaluated against a bioluminescent *Escherichia*

coli (*E. coli*) recombinant strain, used as a model of Gram-negative pathogenic bacteria. The obtained results were compared with the ones previously obtained in our group using the conventional thiopyridinium Pc **7** and **8** (Fig. 3)[13] and are discussed considering the photophysical, photochemical properties of the photosensitizers.

Experimental

All reagents were purchased from Sigma-Aldrich and analytical TLC was carried out on pre-coated silica gel sheets (Merck, 60, 0.2 mm). Molecular extrusion column chromatography was carried out over Bio-beadsTM S-X1 Beads (200-400 Mesh, 100 g), Bio-Rad Laboratories, Inc. ^{1}H and ^{13}C NMR spectra were recorded on a *Bruker Avance-300* spectrometer at 300.13 and 75.47 MHz, respectively, or on a *Bruker Avance-500* at 500.13 and 125.77 MHz. Tetramethylsilane was used as internal reference. The chemical shifts were expressed in δ (ppm) and the coupling constants (J) in Hz. Absorption and fluorescence spectra were recorded using a *Shimadzu UV-2501-PC* and *FluoroMax3* (excitation wavelength of 630 nm, emission range 640–825 nm), respectively. The fluorescence emission spectra of Pc derivatives **3-6** ($C = 1 \times 10^{-6}$ M) were measured in DMF in 1 × 1 cm quartz optical cells under normal air conditions on a computer controlled Horiba Jobin Yvon FluoroMax-3 spectrofluorimeter. The widths of both excitation and emission slits were set at 2.0 nm. The fluorescence quantum yield (Φ_F) of **3-6** was calculated in DMF by comparison of the area below the corrected emission spectra using **ZnPc** as standard ($\lambda_{excitation}$ at 630 nm, $\Phi_f = 0.30$ in DMF).[46] The acquisition of the mass spectra and HRMS were recorded on a *APEXQe FT-ICR* mass spectrometer (Bruker Daltonics, Billerica, MA).

4-(4-Oxopyridin-1(4*H*)-yl)phthalonitrile (1): 4-Fluorophthalonitrile (512.5 mg, 3.5 mmol) and 4-Hydroxypyridine (352.9 mg, 3.7 mmol) were dissolved in 3 mL of dry DMF in a 25 mL round-bottom flask. Some drops of triethylamine were added and the mixture was kept under N_2 atmosphere. The reaction mixture was maintained under stirring for 5 h at 80 ºC, when the TLC control confirmed the consumption of the starting phthalonitrile. Then, the reaction mixture was purified by silica gel column chromatography using a mixture of $CHCl_3$/MeOH (95/5) as eluent. Phthalonitrile **1** (712.3 mg, 3.2 mmol) was obtained in 92% yield, after recrystallization from $CHCl_3$/MeOH. ^{1}H NMR (500 MHz, DMSO-d_6): δ 6.31 (d, J = 7.9 Hz, 2H, H^e), 8.14 – 8.17 (m, 3H, H^{c,d}), 8.33 (d, J = 8.6 Hz, 1H, H^a), 8.50 (d, J = 2.4 Hz, 1H, H^b). ^{13}C NMR (75.5 MHz, DMSO-d_6): δ 112.8, 115.3, 115.5, 116.2, 118.3, 127.1, 127.6, 135.6, 139.0, 145.5, 177.7 (C=O). ESI-MS: *m/z* 222 $[M+H]^+$.

4,5-Bis(4-Oxopyridin-1(4*H*)-yl)phthalonitrile (2): In a 25 mL round-bottom flask, 4,5-Difluorophthalonitrile (300.1 mg, 1.8 mmol) and 4-Hydroxypyridine (356.5 mg, 3.7 mmol) were dissolved in 3 mL of DMF, and then some drops of triethylamine were added. The reaction mixture was maintained under N_2 atmosphere stirring during 5 h at 80 ºC, when the TLC control confirmed the consumption of the starting phthalonitrile. The reaction mixture was purified by silica gel column chromatography using a mixture of $CHCl_3$/MeOH (90/10) as eluent. After evaporation of the solvent, the residue was crystallized from the same mixture of solvents and phthalonitrile **2** (569.3 mg, 1.8 mmol) affording a 99% yield. ^{1}H NMR (500 MHz, DMSO-d_6): δ 6.21 (d, J = 7.9 Hz, 4H, H^c), 7.64 (d, J = 7.9 Hz, 4H, H^b), 8.70 (s, 2H, H^a). ^{13}C NMR (75.5 MHz, DMSO-d_6): δ 114.6, 115.4, 118.3, 133.7, 140.0, 141.2, 177.2 (C=O). ESI-MS: *m/z* 315 $[M+H]^+$.

2,9(10),16(17),23(24)-Tetrakis(4-oxopyridin-1(4*H*)-yl)phthalocyaninatozinc(II) (3): A solution containing phthalonitrile **1** (207.5 mg, 0.9 mmol) and anhydrous zinc chloride (138.9 mg, 1.0 mmol) in 2 mL of 1-pentanol was heated at 140 ºC under N_2 atmosphere in a 25 mL round-bottom flask. After 16 h the reaction was considered to be completed since starting phthalonitrile **1** could no longer be detected by analytic TLC. Chloroform was added and the precipitate was washed several times with the same solvent. The obtained solid was subsequently washed with water in order to remove the excess of zinc chloride. After being dried under vacuum, the crude product was purified by Bio-beadsTM S-X1 column molecular exclusion chromatography using DMF as eluent. The desired product was precipitated from chloroform, filtrated and washed with the same solvent. The Pc **3** (129.5 mg, 0.14 mmol) was isolated in 58% yield. ^{1}H NMR (300 MHz, DMSO-d_6): δ 6.58 – 6.66 (m, 8H, H^e), 8.21 – 8.24 (m, 4H, β-H^c), 8.54 – 8.58 (m, 8H, H^d), 8.96 – 9.05 (m, 8H, α-H^{a,b}). ^{13}C NMR (125.8 MHz, DMSO-d_6): δ 118.1, 118.6, 123.7, 139.8, 140.3, 143.4, 177.8 (C=O). ESI-HRMS *m/z*: calcd for $C_{52}H_{29}N_{12}O_4Zn$: 949,16479 $[M+H]^+$; found: 949,17293 $[M+H]^+$. UV-Vis (DMF), λ_{max} (log ε): 364 (4.48), 613 (4.14), 681 (4.90) nm.

2,3,9,10,16,17,23,24-Octakis(4-oxopyridin-1(4*H*)-yl)phthalocyaninatozinc(II) (4): A solution containing phthalonitrile **2** (310.4 mg, 1.0 mmol) and anhydrous zinc chloride (128.4 mg, 0.9 mmol) in 2 mL of 1-pentanol was heated at 140 ºC under N_2 atmosphere in a 25 mL round-bottom flask. After 16 h the TLC control confirmed that the reaction was complete. The reaction mixture was then precipitated with chloroform, and the solid obtained was washed several times with the same solvent and also with water, in order to remove the excess of zinc chloride. After being dried under vacuum, the crude product was purified by Bio-beadsTM S-X1 column molecular exclusion chromatography using DMF as eluent. The desired product Pc **4** (262.2 mg, 0.2 mmol) was obtained from precipitation with chloroform, filtration and after washing with the same solvent was obtained in 80% yield. ^{1}H NMR (300 MHz, DMSO-d_6): δ 6.36 (d, J = 6.1 Hz, 16H, H^c), 8.13 (d, J = 6.1 Hz, 16H, H^b), 9.63 (s, 8H, α-H^a). ^{13}C NMR (75.5 MHz, DMSO-d_6): δ 118.0, 121.9, 138.3, 139.6, 141.0, 152.3, 176.9 (C=O). ESI-HRMS *m/z*: calcd for $C_{72}H_{40}N_{16}O_8Zn$ 1321,25065 $[M+H]^+$; found: *m/z* 1321,25886 $[M+H]^+$. UV-Vis (DMF), λ_{max} (log ε): 385 (4.81), 616 (4.52), 684 (5.31) nm.

2,9(10),16(17),23(24)-Tetrakis(4-methoxypyridinium-1-yl)phthalocyaninatozinc(II) (5): The pyridinone Pc **3** (103.3 mg, 0.11 mmol) dissolved in 20 mL of dry DMF was added to a large excess of dimethyl sulfate (4 mL, 37.5 mmol). The reaction mixture was kept under stirring overnight at 80 ºC in a sealed tube. The mixture was allowed to cool down and was precipitated with a

mixture of acetone/CH_2Cl_2 (1:1). The obtained residue was filtrated and, after being take

n up in MeOH/H_2O (2:1), was re-precipitated by addition of dichloromethane. The desired product was filtrated, washed with dichloromethane and dried under vacuum. The dark green solid was identified as Pc **5** (110.7 mg, 0.09 mmol) and isolated in 85% yield. ^{1}H NMR (300 MHz, DMSO-d_6): δ 4.29 – 4.54 (m, 12H, OCH_3), 6.69 – 6.75 (m, 4H, β-H^e), 7.99 – 8.15 (m, 8H, H^c), 8.62 – 8.70 (m, 8H, H^d), 9.62 – 9.73 (m, 8H, α-$H^{a,b}$). ^{13}C NMR (125.8 MHz, DMSO-d_6): δ 48.6, 52.9, 58.9, 114.0, 117.9, 146.8, 153, 172.1. UV-Vis (DMF), λ_{max} (log ε): 368 (4.89), 614 (4.66), 680 (5.36) nm; UV-Vis (DMSO), λ_{max} (log ε): 615 (4.70), 682 (5.40) nm; UV-Vis (PBS), λ_{max} (log ε): 624 (4.49) nm. ESI-HRMS *m/z*: calcd for $C_{53}H_{31}N_{12}O_4Zn$: 963.1877; found: 963.1883 $[M\text{-}3CH_3]^{+\bullet}$.

2,3,9,10,16,17,23,24-Octakis(4-methoxypyridinium-1-yl)phthalocyaninatozinc(II) (6): After being dissolved in 20 mL of dry DMF, the pyridinone Pc **4** (106.9 mg, 0.08 mmol) was added to a large excess of dimethyl sulfate (4 mL, 37.5 mmol). The reaction mixture was kept under stirring overnight at 80 ºC in a sealed tube. After this period, the mixture was cooled down and precipitated using a mixture of acetone/CH_2Cl_2 (1/1). The residue obtained was filtrated and re-precipitated by addition of dichloromethane after being taken up in MeOH/H_2O (2:1). The desired product was filtrated, washed with dichloromethane and dried under vacuum. The dark green solid identified as Pc **6** (130.6 mg, 0.07 mmol) was obtained in 88% yield. ^{1}H NMR (300 MHz, DMSO-d_6): δ 4.31 (s, 24H, OCH_3), 7.93 (d, J = 7.1 Hz, 16H, H^c), 9.43 (d, J = 7.1 Hz, 16H, H^b), 10.12 (s, 8H, α-H^a). ^{13}C NMR (125.8 MHz, DMSO-d_6): δ 48.6, 52.9, 59.1, 114.3, 137.6, 139.5, 147.6, 153.0, 172.8. UV-Vis (DMF), λ_{max} (log ε): 634 (4.56), 683 (5.15); UV-Vis (DMSO), λ_{max} (log ε): 616 (4.55), 683 (5.35) nm; UV-Vis (PBS), λ_{max} (log ε): 380 (4.64), 637 (4.10), 675 (5.13) nm. ESI-HRMS *m/z*: calcd for $C_{73}H_{43}N_{16}O_8Zn$: 1335.2736; found: 1335. 2764 $[M\text{-}7CH_3]^{+\bullet}$.

Pc **7** and **8** were prepared according to the literature[13] and present the following spectral absorption features: **Pc 7** UV-Vis (DMSO): λ_{max} (log ε): 352 (4.60), 616 (4.39), 685 (5.20) nm; and **Pc 8** UV-Vis (DMSO) λ_{max} (log ε): 383 (4.55), 630 (4.38), 702 (5.03) nm.

Photosensitizers stock solution. Stock solutions of the photosensitizers used in the photophysical and biological studies were prepared in dimethyl sulfoxide (DMSO) at a concentration of 500 μM, and diluted in DMF/H_2O (9:1), phosphate buffered saline (PBS) or sodium dodecyl sulfate (SDS), depending of the experiments, to obtain the working concentration.

Light source. All the photodynamic inactivation assays were performed under white (400–800 nm) and red (620–750 nm) lights from a compatible fibre optic probe, delivered by a illumination system (LumaCare®, USA, model LC122, with halogen/quartz 250 W lamp) with an irradiance of 150 mW.cm^{-2}and a total light dose of 180 J.cm^{-2}.

Singlet oxygen generation. An aliquot of 3 mL of a solution of the Pc (0.5 μM) and 1,3-diphenylisobenzofuran (DPBF, 50 μM) in DMF/H_2O (9:1) were transferred to a glass cuvette and irradiated with a red light, in order to prevent the photodegradation of DPBF. The red light was delivered by the LED array composed of a matrix of 5 Å~ 5 LED that makes a total of 25 light sources with an emission peak at 640 nm and a bandwidth at half maximum of ± 20 nm. The irradiance was 6.0 mW.cm^{-2} and assays were conducted at room temperature and under gentle magnetic stirring. The absorption of DPBF at 415 nm was measured at defined times with intervals of 15 min. The percentage of the DPBF absorption decay, proportional to the production of $^1O_2$, was assessed by the difference between the initial absorbance and the absorbance of DPBF after irradiation.[47]

Solubility studies. The solubility of new cationic phthalocyanines **5** and **6** in DMSO and PBS was assessed by UV-Vis spectroscopy. Concentrations, between 1 and 20 μM, obtained by the addition of aliquots of each Pc stock solution (500 μM), were analysed. The intensity of the Q-band *versus* Pc concentration was plotted in a graphic for linear regression to determine if these concentrations follow the Beer-Lambert law.

Octanol/water partition coefficient. The octanol/water partition coefficients were determined according with literature[48] by saturating equal volumes of both solvents with the cationic Pc **5** and **6**. For comparison the octanol/water partition coefficients were also determined for Pc **7** and **8** previously synthesized. The obtained results are summarized in table 4. The octanol/water partition coefficients were determined by saturating 1:1 (v/v) mixtures of the solvents with Pc solutions. The mixture was well shook and left overnight to assure that the two phases were completely separated. UV–Vis spectra of the two layers were then taken to measure the last Q-band intensities of the Pc. These data were confirmed by saturating each solvent separately before mixing equal volumes.[49]

Bacterial strain, growth conditions and preparation of stock-suspensions. The bioluminescent *E. coli* Top10 used in these assays was previously obtained by Alves *et al*.[13] and stored at -80 ºC in 10% glycerol until used. Before the photodynamic inactivation assays, a fresh culture in Tryptic Soy Agar (TSA, Liofilchem) with the antibiotics ampicillin (100 mg.mL^{-1}) and chloramphenicol (25 mg.mL^{-1}) was grown for 24 h at 37 ºC. One isolated colony was aseptically inoculated on Tryptic Soy Broth (TSB, Liofilchem) (30 mL) with the antibiotics and grown overnight at 26 ºC under stirring (120 rpm). An aliquot (240 μL) of this culture was sub-cultured in TSB (30 mL) with antibiotics and grown during 20 h at 26 ºC.

PDI experimental setup. Bacterial suspensions, in its early stationary phase (≈10^9 CFU.mL^{-1}) were ten-fold diluted in PBS to a final concentration of ≈10^8 CFU.mL^{-1}. For the experiments, 450 μL of bacterial suspension was aseptically transferred to sterilized 12-well plates and the PS was added from the stock solution to achieve final concentrations of 20 μM. PBS was added to the suspension in order to obtain a final volume of 4.5 mL. After the PS addition, the 12 wells plates were protected from accidental light exposure with an aluminium foil and pre-incubated for 15 min in the dark at room temperature, under stirring (100 rpm), to promote PS binding to *E. coli* cells. After this period, the irradiation was conducted under white and red light during pre-stablished periods (0 (0), 5 (45), 10

(90), 15 (135) and 20 (180) min (J.cm^{-2})). Light and dark controls were included in all the experiments. The light control was conducted without PS. The dark control contained cell suspension at the concentration of 20 μM of PS, but was protected from light with aluminium foil. Three independent assays in triplicate (three aliquots of cell suspension) were conducted for each condition.

Bioluminescence monitoring. In all experiments, aliquots (500 μL) of treated and control samples were collected at time 0, 5, 10, 15 and 20 min of irradiation for bioluminescence measurement in a luminometer (GloMax® 20/20 luminometer).

Photosensitizer binding. Three replicate bioluminescent *E. coli* (10^8 cells.mL^{-1}) suspensions were prepared in PBS and incubated in the dark at room temperature in the presence of 20 μM of each PS. After 15 min of incubation, unbound PS was removed from the suspension by centrifugation for 5 min, at 13,000 *g* (Hettich Mikro 120). Pellets were further washed with PBS + 5% DMSO, digested in 1 mL of a solution containing 2% SDS (Merck) and 0.1 M of NaOH (Scharlau) and incubated at room temperature for 24 h or until to obtain a clear solution. The fluorescence of the extracts was measured on a *FluoroMax3* spectrofluorimeter with a slit of 2 nm. The excitation wavelengths for all compounds were 630 nm. The range for emission was 640 to 825 nm. The measured fluorescence intensity allowed the determination of the corresponding PS concentration by interpolation with a calibration plot built with known concentrations of each PS, using the digestion solution as solvent. Parallel aliquots of cell suspensions incubated in the presence of the PS were read and log luminescence (RLU) was assessed. The adsorption value was calculated according to the literature.[50] Three independent assays were performed for each combination of bacterial strain PS.

Statistical analysis. Statistical analysis was performed in SPSS 15.0 for Windows (SPSS Inc., USA). The significance of the PDI effect of each PS and of the irradiation time on bacterial cells viability was assessed by an unvaried analysis of variance (ANOVA) model with the Bonferroni post hoc test. Normal distributions were assessed by the Kolmogorov–Smirnov test and homogeneity of variances was assessed by the Levene test. A value of $p < 0.05$ was considered significant.

Results and Discussion

Synthesis of pyridinone Pc and precursors

A simple access to obtain the new amphiphilic methoxypyridinium Pc conjugates **5** and **6** is summarized in Scheme 1. The synthetic strategy required the previous preparation of the new pyridinone phthalonitrile derivatives **1** and **2**; these phthalonitriles were isolated in excellent yields (higher than 90%) from reaction of 4-Hydroxypyridine with the adequate fluorophthalonitriles. The tetramerization of these synthons in presence of zinc(II) chloride afforded the expected tetra- and octa-pyridinone Pc **3** and **4** in yields higher than 58%. The subsequent methylation of these dyes in the presence of a large excess of dimethyl sulfate in DMF at 80 ºC, gave rise to the corresponding cationic Pc **5** and **6** in yields higher than 80%. The structures of phthalonitriles **1** and **2** and of Pc **3**-**6** were confirmed by NMR (Figs. S1-14) and by mass spectrometry (Figs. S15-20).

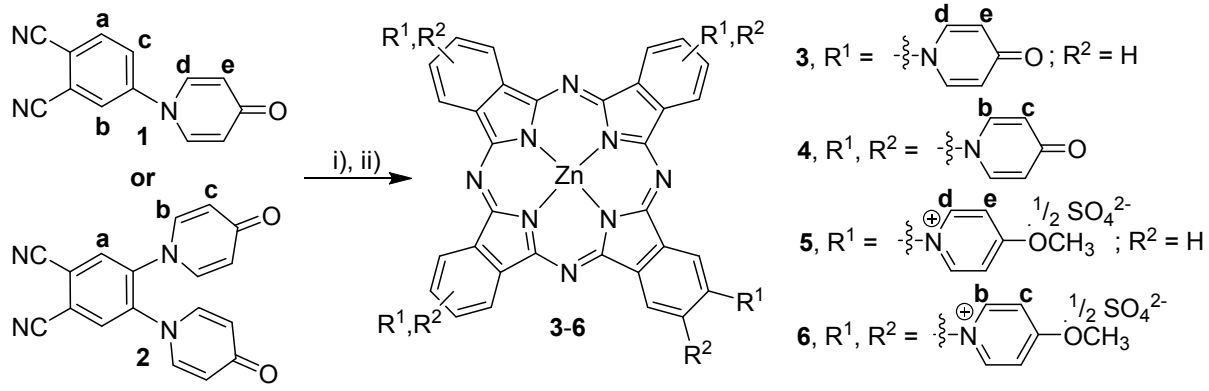

i) $ZnCl_2$, 1-pentanol, 140 ºC, 16 h; ii) $(CH_3)_2SO_4$, DMF, 80 ºC, 24 h.

Scheme 1

The main photophysical features of Pc **3**-**6** such as Q-band wavelengths, molar extinction coefficients (ε), fluorescence emission wavelength ($\lambda_{emission}$), Stokes shift and fluorescence quantum yields (Φ_F) – are summarized in table 1. These Pc show the characteristic absorption features expected for metallic phthalocyanine complexes – a rather weak absorption Soret-band in the region of 300-425 nm and a strong Q-band maximum at 680-684 nm (Fig. 1). Considering the excited state all the Pc upon excitation at 630 nm in DMF show a band with a maximum at 688 nm (see also Fig. 1). The values of the quantum yields in DMF vary between 0.09-0.24 and are slight lower than the one of **ZnPc** (0.30)[46] used as reference in the same solvent.

Solubility

UV-Vis absorption spectra acquired in PBS and DMSO are displayed in figure 2. Both cationic PS **5** and **6** showed typical absorption spectra in DMSO, with two well-defined Q-bands at 605

and 677 nm. However, a visible change is observed in the UV-Vis spectra when PBS was used as solvent. In the case of PS **5**, the two Q-bands became a broad band with maximum absorbance at 610 nm and an intense Soret-band, indicative of aggregation in PBS. The PS **6** shows slight blue shift of both bands but still sharp, which is an evidence of good solubility in PBS. Although the solubility studies relying on Beer-Lambert law, determined in DMSO and PBS (Fig. S21), did not show aggregation behaviour for concentrations bellow 20 and 5 μM, respectively, a notorious aggregation of PS **5**, in PBS after a pre-incubation period of 15 min in the dark was observed, using the same experimental conditions as in the PDI assays (20 μM) (Fig. S22).

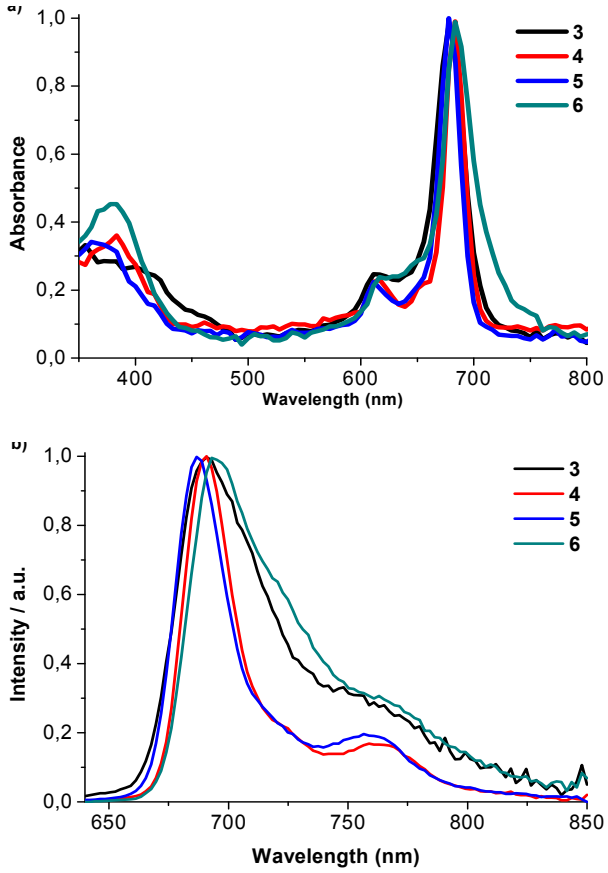

Fig. 1 – Normalized a) absorption and b) emission spectra (at excitation of 630 nm) of Pc derivatives **3-6** in DMF.

Table 1. Photophysical properties of Pc derivatives **3-6** in DMF.

Compound	Q-band λ_{max} (nm)	log ε	$\lambda_{emission}$ (nm)[a)]	Stokes shift (nm)	Φ_F[b)]
3	677	4.90	690	13	0.07
4	683	5.31	690	7	0.26
5	677	5.36	687	10	0.30
6	683	4.56	693	10	0.17

[a)]excited at 630 nm; [b)]using **ZnPc** in DMF as reference (Φ_F = 0.30).[46]

Octanol/water partition coefficient

The octanol/water partition coefficients were determined by UV-Vis spectra (data not shown) according with literature by saturating equal volumes of both solvents with the cationic Pc **5** and **6**. For comparison the octanol/water partition coefficients of Pc **7** and **8** previously prepared (Fig. 3)[13] were also determined. The obtained results are summarized in table 4 and show that the position of the charge and the presence of the thiopyridinium or inverted methoxypyridinium moiety influence considerably the aqueous solubility. Pc **5** shows lower solubility, compared with the Pc **6-8**, taken in consideration the analysis of the partition coefficient in octanol/water (Table 2). The obtained results show that the thiopyridinium Pcs are more soluble in pure water than the methoxypyridinium Pcs.

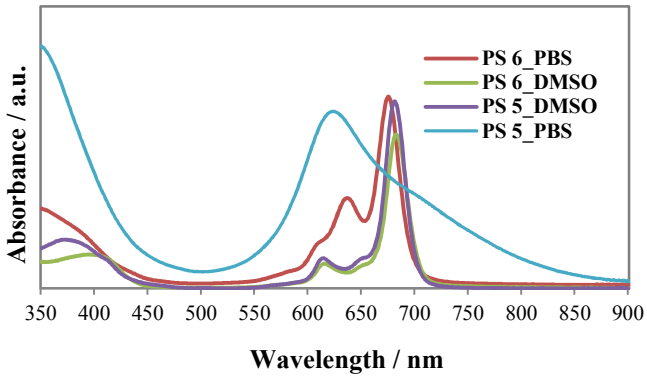

Fig. 2 – Absorption spectra of **5** and **6** in DMSO and PBS (1 μM).

Table 2. Octanol/water partition coefficient of cationic Pc **5-8**.

Compound	Log $P_{o/w}$
5	-2.80
6	-4.02
7	-4.00
8	-4.24

Singlet oxygen generation

The absorption decay of a solution of 1,3-diphenylisobenzofuran (DPBF) in the presence of the different PS, allowed a qualitative evaluation of the ability of these cationic PS **5**, **6** and of the thiopyridinium phthalocyanines **7** and **8** (Fig. 4) to generate singlet oxygen ($^1O_2$). Both methoxypyridinium PS **5** and **6** and thiopyridinium PS **7** proved to be efficient $^1O_2$ generators (92, 37 and 76% of DPBF decay, after 5 min of irradiation respectively) in DMF/H_2O (9:1). Pc **5** shows the highest $^1O_2$ generation. On the contrary, Pc **8**, under the same experimental conditions, caused only 9% of DPBF absorbance decay, being the less efficient singlet oxygen generator in the conditions tested.

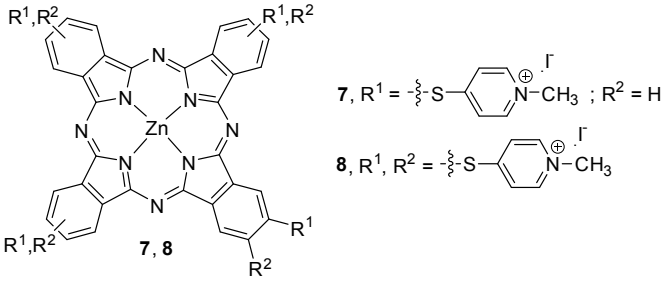

Fig. 3 – Structures of thiopyridinium Pc **7** and **8** used as comparison to **5** and **6** in the PDI assays, against bioluminescent *E. coli.*

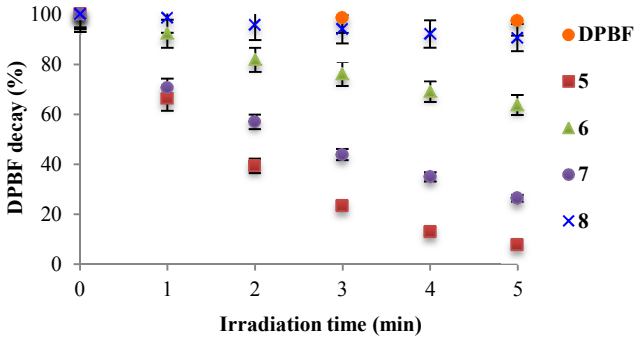

Fig. 4 – Time-dependent decomposition of DPBF (50 μM) photosensitized by PS **5-8** in DMF/H_2O (9:1) upon irradiation with a LED array system (640 nm ± 20 nm) at an irradiance of 6.0 mW.cm^{-2} with or without PS (0.5 μM).

Photodynamic inactivation of *Escherichia coli*

The inactivation kinetics of *E. coli* with artificial white and red lights, in the presence of Pc **5-8**, is shown in figure 5. The two controls, light and dark (LC and DC, respectively) were also included. The viability of bioluminescent *E. coli* was not affected (ANOVA, p > 0.05) neither by irradiation alone (LC) nor by the PS used at 20 μM in the absence of light (DC).

a)

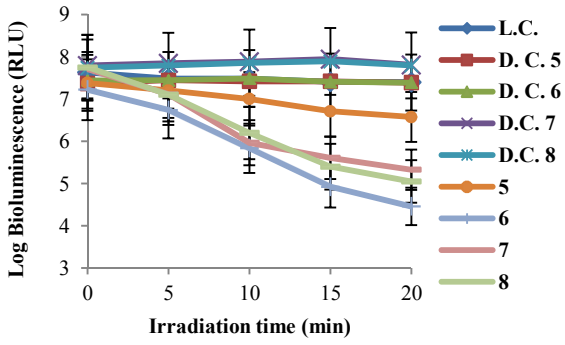

b)

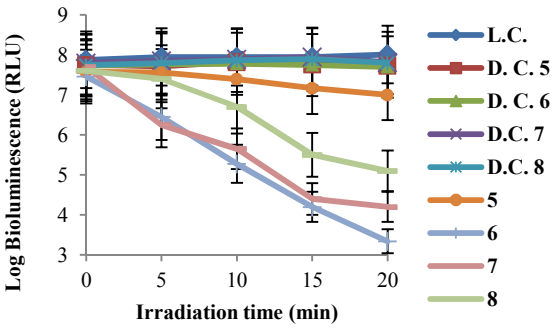

Fig. 5 – Survival of bioluminescent *E. coli* during PDI experiments with 20 μM of Pc **5-8**, after irradiation with a) white light (400–800 nm) and b) red light (620–750 nm) at an irradiance of 150 mW.cm^{-2}, during 20 min (between 0 and 180 J.cm^{-2}). Values correspond to the average of 3 independent experiments in duplicate. Error bars represent standard deviation.

Upon irradiation with white light (Fig. 5a) PSs **6**, **7** and **8** caused significantly higher inactivation (2.8, 2.3 and 2.7 logs of reduction in bioluminescence emission (ANOVA, $p < 0.05$) than PS **5** (0.8 log reduction in bioluminescence emission (ANOVA, $p > 0.05$), after 20 min of irradiation. In the assays with red light (Fig. 5b), three distinct profiles were observed. Once again, PS **5** showed significantly lower inactivation efficiency (0.9 log of reduction in bioluminescence emission (ANOVA, $p < 0.05$) followed by PS **8** (2.3 log of reduction in bioluminescence emission) (ANOVA, $p < 0.05$). The inactivation profiles of PS **6** and **7** were very similar during the initial 15 min of irradiation (3.5 log of reduction in bioluminescence emission). However, during the last 5 min of irradiation, PS **7** inactivation stabilized, while PS **6** photoinactivation progressed to a final 4.1 log of reduction in bioluminescence emission.

Comparing the PDI efficiency obtained under the two light conditions, red light enhanced photodynamic inactivation with PS **6** and **7** (ANOVA, $p < 0.05$), while for PS **8** the wavelength of the irradiation light did not improve its bacterial photodynamic inactivation efficiency.

Photosensitizer binding

The amount of PS bound to *E. coli* cells after 15 min of incubation in the dark with 20 μM of PS, are summarized in figure 6. The methoxypyridinium PS **5** was significantly more retained by bacterial cells (1.40 × 10^8 PS molecules CFU.mL^{-1}, ANOVA, $p < 0.05$) than the other tested PS. Methoxypyridinium PS **6** and thiopyridinium PS **7** presented binding values in order of 3.46 × 10^6 and 5.49 × 10^6 PS molecules CFU.mL^{-1}, respectively. Thiopyridinium PS **8** presented the lowest binding value (1.35 × 10^6 PS molecules CFU.mL^{-1}).

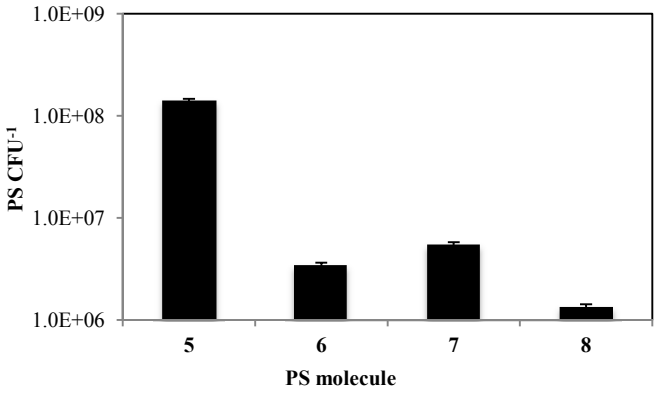

Fig. 6 – Binding of cationic PSs **5-8** (20 μM) by the bioluminescent *E. coli* cells after 15 min of incubation in dark at room temperature. Values correspond to the average of 3 independent experiments. Error bars represent standard deviation.

DISCUSSION

The search for new PS with suitable features for inactivation of clinical pathogenic agents has led to the development of new second-generation molecules based on phthalocyanines due to their high absorption in the red region of the electromagnetic spectrum. However, in order to improve the interaction of the Gram-negative membranes with the PS the presence of cationic charges in PS core is an important feature. In here it is described an easy synthetic access to the new tetra- and octa-methoxypyridinium Pc **5** and **6** and based on their photochemical and photophysical features their efficiency to photoinactivate a Gram-negative bacterial strain bioluminescent *E. coli* were evaluated. The efficiency of these new PSs was compared with the efficiency of previously prepared phthalocyanines **7** and **8**. The use of cationic Pc with trimethylammonium[51,52] or even pyridinium groups[13] as antimicrobial agents has already been described.

The two cationic phthalocyanines **5** and **6** were obtained by tetramerization of pyridinone phthalonitrile derivatives **1** and **2**, followed by *O*-methylation of the corresponding pyridinone Pc dyes **3** and **4** (Scheme 1). The pyridinone phthalonitrile derivatives **1** and **2** were obtained by nucleophilic substitution of adequate functionalized nitro phthalonitriles with 4-hydroxypyridine. The access to this interesting inverted methoxypyridinium phthalocyanines can be justified by the presence of a high content of the tautomer pyridinone in equilibrium with 4-hydroxypyridine. In fact, previous results have shown that the tetra-substitution of 5,10,15,20-tetrakis-(2,3,4,5,6-pentafluorophenyl)-porphyrin (**$TPPF_{20}$**) results in a 4-pyridinone derivative.[53-56]

Factors like substitution type, that affect PS binding, and photophysical features are determinants of the PS photosensitization efficiency against bacterial cells.[57] Singlet oxygen ($^1O_2$) production, water solubility, octanol/water partition coefficient and binding studies were conducted in order to understand the photosensitization performance of the tetra- (**5** and **7**) and octa-cationic (**6** and **8**) Pc. $^1O_2$ is the major reactive oxygen species (ROS) produced by this kind of macrocycles during PDI, being the intermediate for cell damage and subsequent death.[8,15,17] In this study, PS **5** at the same concentration (0.5 μM) showed significantly higher $^1O_2$ production when compared to the other molecules (Fig. 4). However, a higher PDI efficiency was not observed, regardless the light source used, indicating that $^1O_2$ production yield is not the sole determinant of the efficiency of photodynamic inactivation of bacterial cells; this fact can be related to aggregation of PS **5** during the PDI assays, conducted in buffer solution (PBS), even with 5% of DMSO. Aggregated molecules lose their monomeric form and some of their physical-chemical features, which reduces PDI efficiency. Aggregation in aqueous medium may also underlie, as an artefact, the apparently higher PS **5** binding to bacterial cells. In fact, this hypothesis is supported by the partition coefficient (o/w) value, where PS **5** presents a higher affinity to the organic phase, when compared to the other PS tested (**6-8**). Although PS **6-8** displayed similar partition coefficients, higher than PS **5**, revealing a good affinity to aqueous media, they behaved differently as to the PDI efficiency.

Despite the lower $^1O_2$ production and binding values of PS **8**, it was observed a PDI efficiency similar to PS **6** and **7**, when irradiated with white light. However, unlike PS **6** and **7**, its efficiency did not increase with red light. The photodynamic inactivation potential of PS **7** and **8** confirm that water solubility, $^1O_2$ production and affinity to cellular material, taken together, significant modulate the overall performance of a PS for antimicrobial photodynamic approaches. However, other photophysical and chemical aspects are also relevant. PS **6** presented higher $^1O_2$ production and binding affinity than PS **7**, and similar partition coefficients but the later was more efficient in PDI under red light. This can be explained by the complete overlapping of PS **6** Q-band into the red light emission used (620-750 nm, Fig. 7), compared to the PS **7**. The light wavelength necessary to induce photosensitization depends on the electronic absorption spectrum of the PS and the emission spectrum of the light source.[58] The small differences in the PDI efficiency with PS **6** and **7** under white light, could be related to different affinity to outer bacterial structures.

It is also important to highlight that the structural manner in which hydroxypyridine is bound to the Pc core, may also influence the PDI performance. The substitution by the nitrogen instead of thio-bridge, like in PS **7** and **8**, probably makes the former less flexible. In addition, the position of the positive charge may also contribute to the aggregation behaviour in water, once it is more protected from the surrounding environment.

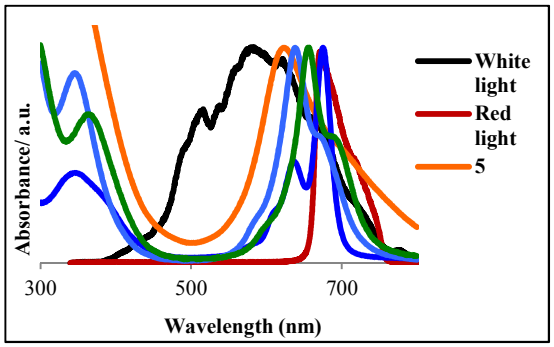

Fig. 7 – Normalized UV-Vis spectra of Pc **5-8** in PBS with white and red light source emission spectra.

Charge number is another essential driver of PS affinity toward cellular targets critical for the stability of cell organization and⁄or function.[59,60] A high number of positive charges was hypothesized to result in reduced photosensitization efficiency.[39,50] However, in the present work, the best PS had different charge numbers: eight (in PS **6**) and four (in PS **7**). Again, the results indicate that PDI efficiency is determined by a complex interplay of photophysical, chemical and biological photosensitizer features.

Conclusions

Novel pyridinone and methoxypyridinium Pc derivatives **3-6** were prepared and structurally characterized by NMR spectroscopy and mass spectrometry. Pc derivative **6** proved to be the best efficient photosensitizer against bioluminescent recombinant strain of *E. coli*, due to the conjunction of octanol/water partition coefficient, $^1O_2$ production and good overlap between the PS absorbance spectrum and lights source emission. The affinity form of PS **6** to the outer bacterial structures, which the methoxypyridinium moieties are less flexible comparing with the thiopyridinium groups of PS **7** and **8**, would be also important in the PDI result. The type, number and position of the positive charged play a key role in the physicochemical and biological features of the phthalocyanine derivatives, confirming that these characteristics should be further addressed in the pursue for optimized PS for PDI of microbial pathogens.

Acknowledgements

Thanks are due to the University of Aveiro, FCT (Portugal), European Union, QREN, FEDER and COMPETE for funding QOPNA Research Unit (Project PEst-C/QUI/UI0062/2013; FCOMP-01-0124-FEDER-037296), the Portuguese National NMR Network. Leandro M. O. Lourenço (SFRH/BD/64526/2009) and Maria C. Gomes (SFRH/BD/88334/2012) thank FCT for their Ph.D. grants. J. Tomé thanks FCT for the grant PTDC/CTM/101538/2008.

Notes and references

[a]*Department of Chemistry and QOPNA, University of Aveiro, 3810-193 Aveiro, Portugal*
[b]*Department of Biology and CESAM, University of Aveiro, 3810-193 Aveiro, Portugal*
[c]*Department of Organic and Macromolecular Chemistry, Ghent University, B-9000 Gent, Belgium.*

[a] † Footnotes should appear here. These might include comments relevant to but not central to the matter under discussion, limited experimental and spectral data, and crystallographic data.
Electronic Supplementary Information (ESI) available: [details of any supplementary information available should be included here]. See DOI: 10.1039/b000000x/

1. McKeown, N. B., in The Porphyrin Handbook, *The synthesis of symmetrical phthalocyanines*, Kadish, K. M., K. M. Smith and R. Guilard, Eds., Academic Press, New York, NY, USA, vol. 15, cap. 98, pp. 61–124, 2003.
2. Lyubimtsev, A., Z. Iqbal, G. Crucius, S. Syrbua, T. Ziegler and T. Hanack (2012) Synthesis of glycosylated metal phthalocyanines and naphthalocyanines. *J. Porphyrins Phthalocyanines*. **16**, 434–463.
3. Lourenço, L. M. O., M. G. P. M. S. Neves, J. A. S. Cavaleiro and J. P. C. Tomé, (2014) Synthetic approaches to glycophthalocyanines. *Tetrahedron*. **70**, 2681–2698.
4. Wibmer, L., L. M. O. Lourenço, A. Roth, G. Katsukis, M. G. P. M. S. Neves, J. A. S. Cavaleiro, J. P. C. Tomé, T. Torres and D. M. Guldi (2015) Decorating graphene nanosheets with electron accepting pyridyl phthalocyanines, *Nanoscale*, DOI: 10.1039/C4NR05719H.
5. Berthold, H. J., S. Franke, J. Thiem and T. Schotten (2010) Ex Post Glycoconjugation of Phthalocyanines. *J. Org. Chem*. **75**, 3859–3862.
6. Lourenço, L. M. O., P. M. R. Pereira, E. Maciel, M. R. M. Domingues, R. Fernandes, M. G. P. M. S. Neves, J. A. S. Cavaleiro and J. P. C. Tomé (2014) Amphiphilic phthalocyanine–cyclodextrin conjugates for cancer photodynamic therapy. *Chem. Comm*. **50**, 8363–8366.
7. Soares, A. R., M. G. P. M. S. Neves, A. C. Tomé, M. C. Iglesias-de la Cruz, A. Zamarron, E. Carrasco, S. Gonzalez, J. A. S. Cavaleiro, T. Torres, D. M. Guldi and A. Juarranz (2012) Glycophthalocyanines as Photosensitizers for Triggering Mitotic Catastrophe and Apoptosis in Cancer Cells. *Chem. Res. Toxicol*. **25**, 940–951.
8. Silva, S., P. M. R. Pereira, P. Silva, F. A. A. Paz, M. A. F. Faustino, J. A. S. Cavaleiro and J. P. C. Tomé (2012) Porphyrin and phthalocyanine glycodendritic conjugates: synthesis, photophysical and photochemical properties. *Chem. Commun*. **48**, 3608–3610.
9. Pereira, P. M. R., S. Silva, J. A. S. Cavaleiro, C. A. F. Ribeiro, J. P. C. Tomé and R. Fernandes (2014) Galactodendritic Phthalocyanine Targets Carbohydrate-Binding Proteins Enhancing Photodynamic Therapy. *PLOS One*. **9**, 1–13.
10. Bolfarini, G. C., M. P. Siqueira-Moura, G. J. F. Demets, P. C. Morais and A. C. Tedesco (2012) In vitro evaluation of combined hyperthermia and photodynamic effects using magnetoliposomes loaded with cucurbituril zinc phthalocyanine complex on melanoma. *J. Photochem. Photobiol., B*. **115**, 1–4.
11. Bolfarini, G. C., M. P. Siqueira-Moura, G. J. F. Demets and A. C. Tedesco (2014) Preparation, characterization, and in vitro phototoxic effect of zinc phthalocyanine cucurbit[7]uril complex encapsulated into liposomes. *Dyes Pigm*. **100**, 162–167.
12. Huang, J.-D., S. Wang, P.-C. Lo, W.-P. Fong, W.-H. Kod and D. K. P. Ng (2004) Halogenated silicon(IV) phthalocyanines with axial poly(ethylene glycol) chains. Synthesis, spectroscopic properties, complexation with bovine serum albumin and in vitro photodynamic activities. *New J. Chem*. **28**, 348–354.
13. Pereira, J. B., E. F. A. Carvalho, M. A. F. Faustino, M. G. P. M. S. Neves, J. A. S. Cavaleiro, N. C. M. Gomes, Â. Cunha, A. Almeida and J. P. C. Tomé (2012) Phthalocyanine Thio-Pyridinium Derivatives as Antibacterial Photosensitizers. *Photochem. Photobiol*. **88**, 537–547.
14. Almeida, A., Â. Cunha, M. A. F. Faustino, A. C. Tomé, M. G. P. M. S. Neves, in Photodynamic Inactivation of Microbial Pathogens, Medical and Environmental Applications, *Porphyrins as Antimicrobial Photosensitizing Agents*, Hamblin, M. R. and G. Jori, Eds., RSC Publishing: Cambridge, England, Chapter 5, pp. 83–160, 2011.

15. Mikula, P., L. Kalhotka, D. Jancula, S. Zezulka, R. Korinkova, J. Cerny, B. Marsalek and P. Toman (2014) Evaluation of antibacterial properties of novel phthalocyanines against Escherichia coli – Comparison of analytical methods. *J. Photochem. Photobiol*., B. **138**, 230–239.
16. Osifeko, O. L. and T. Nyokong (2014) Applications of lead phthalocyanines embedded in electrospun fibers for the photoinactivation of *Escherichia coli* in water. *Dyes Pigm*. **111**, 8-15.
17. Managa, M., M. A. Idowu, E. Antunes and T. Nyokong (2014) Photophysicochemical behavior and antimicrobial activity of dihydroxosilicon tris(diaquaplatinum)octacarboxyphthalocyanine. *Spectrochim. Acta, Part A*. **125**,147–153.
18. CIBA Foundation Symposium, Photosensitizing Compounds: Their Chemistry, Biology and Clinical Use; G. Bock and S. Harnett, Eds., John Wiley: Chichester, UK, vol. 727, pp. 1–32 and 60–130, 2008.
19. Dumoulin, F., M. Durmuş, V. Ahsen and T. Nyokong (2010) Synthetic pathways to water-soluble phthalocyanines and close analogs. *Coord. Chem. Rev*. **254**, 2792–2847.
20. Ghani, F., J. Kristen and H. Riegler (2012) Solubility Properties of Unsubstituted Metal Phthalocyanines in Different Types of Solvents. *J. Chem. Eng. Data*. **57**, 439−449.
21. Masilela, N. and T. Nyokong (2010) The synthesis and photophysical properties of novel cationic tetra pyridiloxy substituted aluminium, silicon and titanium phthalocyanines in water. *J. Lumin*. **130**, 1787–1793.
22. Durmus, M. and T. Nyokong (2007) Synthesis, photophysical and photochemical properties of aryloxy tetra-substituted gallium and indium phthalocyanine derivatives. *Tetrahedron*. **63**, 1385–1394.
23. Oleinick, N. L., A. R. Antunez, M. E. Clay, B. D. Rihter and M. E. Kenney (1993) New phthalocyanine photosensitizers for photodynamic therapy. *Photochem. Photobiol*. **57**, 242–247.
24. Zamora-León, S. P., D. W. Golde, I. I. Concha, C. I. Rivas, F. Delgado-Lopez, J. Baselga, F. Nualart and J. C. Vera (1996) Expression of the fructose transporter GLUT5 in human breast cancer. *Proc. Natl. Acad. Sci. U.S.A*. **93**, 1847–1852.
25. Chandler, J. D., E. D. Williams, J. L. Slavin, J. D. Bestand and S. Rogers (2003) Expression and localization of GLUT1 and GLUT12 in prostate carcinoma. *Cancer*. **97**, 2035–2042.
26. Lo, P.-C., J.-D. Huang, D. Y. Y. Cheng, E. Y. M. Chan, W.-P. Fong, W.-H. Ko and D. K. P. Ng (2014) New Amphiphilic Silicon(IV) Phthalocyanines as Efficient Photosensitizers for Photodynamic Therapy: Synthesis, Photophysical Properties, and in vitro Photodynamic Activities. *Chem. Eur. J*. **10**, 4831–4838.
27. Leng, X., C.-F. Choi, P.-C. Lo and D. K. P. Ng (2007) Assembling a Mixed Phthalocyanine−Porphyrin Array in Aqueous Media through Host−Guest Interactions. *Org. Lett*. **9**, 231–234.
28. Hofman, J.-W., F. V. Zeeland, S. Turker, H. Talsma, S. A. G. Lambrechts, D. V. Sakharov, W. E. Hennink and C. F. V. Nostrum (2007) Peripheral and axial substitution of phthalocyanines with solketal groups: synthesis and in vitro evaluation for photodynamic therapy. *J. Med. Chem*. **50**, 1485–1494.
29. Lee, P. P. S., P. C. Lo, E. Y. M. Chan, W. P. Fong, W. H. Ko and D. K. P. Ng (2005) Synthesis and in vitro photodynamic activity of novel galactose-containing phthalocyanines. *Tetrahedron Lett*. **46**, 1551–1554.
30. Peng, Q., in Photodynamic Therapy and Fluorescence Diagnosis in Dermatology, *Correlation of intracellular and intratumoural photosensitizer distribution with photodynamic effect*, Calzavara-Pinton, P. G., R. M. Szeimies and B. Ortel, Eds., Elsevier, Amsterdam, pp. 55–66, 2001.
31. Mantareva, V., V. Kussovski, I. Angelov, E. Borisova, L. Avramov, G. Schnurpfeil and D. Wöhrle (2007) Photodynamic activity of water-soluble phthalocyanine zinc(II) complexes against pathogenic microorganisms. *Bioorg. Med. Chem*. **15**, 4829–4835.
32. Fu, X.-J., Y. Fang and M. Yao (2013) Antimicrobial Photodynamic Therapy for Methicillin-Resistant Staphylococcus aureus Infection. *BioMed Res. Int*. **2013**, 1–9.
33. Pereira, M. A., M. A. F. Faustino, J. P. C. Tomé, M. G. P. M. S. Neves, A. C. Tomé, J. A. S. Cavaleiro, Â. Cunha and A. Almeida (2014) Influence of external bacterial structures in the efficiency of photodynamic inactivation by a cationic porphyrin. *Photochem. Photobiol. Sci*. **13**, 680–690.
34. Ke, M.-R., J. M. Eastel, K. L. K. Ngai, Y.-Y. Cheung, P. K. S. Chan, M. Hui, D. K. P. Ng and P.-C. Lo (2014) Photodynamic inactivation of bacteria and viruses using two monosubstituted zinc(II) phthalocyanines. *Eur. J. Med. Chem*., **84**, 278–283.
35. Spesia, M. B., M. Rovera and E. N. Durantini (2010) Photodynamic inactivation of Escherichia coli and Streptococcus mitis by cationic zinc(II) phthalocyanines in media with blood derivatives. *Eur. J. Med. Chem*. **45**, 2198–2205.
36. Junqueira, J. C., A. O. C. Jorge, J. O. Barbosa, R. D. Rossoni, S. F. G. Vilela, F. A. C. B. P. Costa, L. Primo, J. M. Gonçalves, A. C. Tedesco and J. M. A. H. Suleiman (2012) Photodynamic inactivation of biofilms formed by Candida spp., Trichosporon mucoides, and Kodamaea ohmeri by cationic nanoemulsion of zinc 2,9,16,23-tetrakis(phenylthio)-29H, 31H-phthalocyanine (ZnPc). *Lasers Med. Sci*. **27**, 1205–1212.
37. Alves, E., C. M. B. Carvalho, J. P. C. Tomé, M. A. F. Faustino, M. G. P. M. S. Neves, A. C. Tomé, J. A. S. Cavaleiro, Â. Cunha, S. Mendo and A. Almeida (2008) Photodynamic inactivation of recombinant bioluminescent Escherichia coli by cationic porphyrins under artificial and solar irradiation. *J. Ind. Microbiol. Biotechnol*. **35**, 1447–1454.
38. Alves, E., L. Costa, C. M. B. Carvalho, J. P. C. Tomé, M. A. F. Faustino, M. G. P. M. S. Neves, A. C. Tomé, J. A. C. Cavaleiro, Â. Cunha and A. Almeida (2009) Charge effect on the photoinactivation of Gram-negative and Gram-positive bacteria by cationic meso-substituted porphyrins. *BMC Microbiol.*, **9**, 1–13.
39. Schastak, S., S. Ziganshyna, B. Gitter, P. Wiedemann and T. Claudepierre (2010) Efficient Photodynamic Therapy against Gram-Positive and Gram-Negative Bacteria Using THPTS, a Cationic Photosensitizer Excited by Infrared Wavelength. *PLoS ONE*, **5**, 1–8.
40. Malik, Z., H. Ladan and Y. Nitzan (1992) Photodynamic inactivation of Gram-negative bacteria: problems and possible solutions. *J. Photochem. Photobiol. B*. **14**, 262–266.
41. Kuznetsova, N. A., D. A. Makarov, O. L. Kaliya and G. N. Vorozhtsov (2007) Photosensitized oxidation by dioxygen as the base for drinking water disinfection. *J. Hazard. Mater*. **146**, 487–491.
42. Taraszkiewicz, A., M. Grinholc, K. P. Bielawski, A. Kawiak and J. Nakonieczna (2013) Imidazoacridinone Derivatives as Efficient Sensitizers in Photoantimicrobial Chemotherapy. *Appl. Environ. Microbiol*. **79**, 3692–3702.

43. Mesquita, M. Q. , J. C. J. M. D. S. Menezes, M. G. P. M. S. Neves, A. C. Tomé, J. A. S. Cavaleiro, Â. Cunha, A. Almeida, S. Hackbarth, B. Röder and M. A. F. Faustino (2014) Photodynamic inactivation of bioluminescent Escherichia coli by neutral and cationic pyrrolidine-fused chlorins and isobacteriochlorins. *Bioorg. Med. Chem. Lett*. **24**, 808–812.
44. Mesquita, M. Q., J. C. J. M. D. S. Menezes, S. M. G. Pires, M. G. P. M. S. Neves, M. M. Q. Simões, A. C. Tomé, J. A. S. Cavaleiro, Â. Cunha, A. Almeida, A. L. Daniel-da-Silva and M. A. F. Faustino (2014) Pyrrolidine-fused chlorin photosensitizer immobilized on solid supports for the photoinactivation of Gram negative bacteria. *Dyes Pigm*. **110**, 123–133.
45. Almeida, J., J. P. C. Tomé, M. G. P. M. S. Neves, A. C. Tomé, J. A. S. Cavaleiro, A. Cunha, L. Costa, M. A. F. Faustino and A. Almeida (2014) Photodynamic inactivation of multidrug-resistant bacteria in hospital wastewaters: influence of residual antibiotics. *Photochem. Photobiol. Sci*. **13**, 626–633.
46. Vincett, P. S., E. M. Voigt and K. E. Rieckhoff (1971) Phosphorescence and Fluorescence of Phthalocyanines. *J. Chem. Phys*. **55**, 4131–4140.
47. Pereira, P. M. R., J. J. Carvalho, S. Silva, J. A. S. Cavaleiro, R. J. Schneider, R. Fernandes and J. P. C. Tomé (2014) Porphyrin conjugated with serum albumins and monoclonal antibodies boosts efficiency in targeted destruction of human bladder cancer cells. *Org. Biomol. Chem.* **12**, 1804–1811.
48. Sangster, J., (1989) Octanol-Water Partition Coefficients of Simple Organic Compounds. *J. Phys. Chem. Ref. Data*. **18**, 1111–1227.
49. Aggarwal, A., S. Thompson, S. Singh, B. Newton, A. Moore, R. Gao, X. Gu, S. Mukherjee and C. M. Drain (2014) Photophysics of Glycosylated Derivatives of a Chlorin, Isobacteriochlorin and Bacteriochlorin for Photodynamic Theragnostics: Discovery of a Two-photon-absorbing Photosensitizer. *Photochem. Photobiol*., **90**, 419–430.
50. Demidova, T. N. and M. R. Hamblin (2005) Photodynamic Inactivation of Bacillus Spores, Mediated by Phenothiazinium Dyes. *Appl. Environ. Microbiol.* **71**, 6918–6925.
51. Segalla, A., C. D. Borsarelli, S. E. Braslavsky, J. D. Spikes, G. Roncucci, D. Dei, G. Chiti, G. Jori and E. Reddi (2002) Photophysical, photochemical and antibacterial photosensitizing properties of a novel octacationic Zn(II)-phthalocyanine. *Photochem. Photobiol. Sci.* 1, 641–648.
52. Soncin, M., C. Fabris, A. Busetti, D. Dei, D. Nistri, G. Roncucci and G. Jori (2002) Approaches to selectivity in the Zn(II)–phthalocyanine-photosensitized inactivation of wild-type and antibiotic-resistant Staphylococcus aureus. *Photochem. Photobiol. Sci.* **1**, 815–819.
53. Costa, D. C. S., V. F. Pais, A. M. S. Silva, J. A. S. Cavaleiro, U. Pischel and J. P. C. Tomé (2014) Cationic porphyrins with inverted pyridinium groups and their fluorescence properties. *Tetrahedron. Lett*. **55**, 4156–4159.
54. Kocak, A. and S. Kurbanli (2007) Synthetic Communications: An International Journal for Rapid Communication of Synthetic Organic Chemistry. *Synth. Commun*. **37**, 3697–3708.
55. Khan, T. K., M. R. Rao and M. Ravikanth (2010) Synthesis and Photophysical Properties of 3,5-Bis(oxopyridinyl)- and 3,5-Bis(pyridinyloxy)-Substituted Boron-Dipyrromethenes. *Eur. J. Org. Chem*. **12**, 2314–2323.
56. Samaroo, D., M. Vinodu, X. Chen and C. M. Drain (2007) meso-Tetra(pentafluorophenyl)porphyrin as an efficient platform for combinatorial synthesis and the selection of new photodynamic therapeutics using a cancer cell line. *J. Comb. Chem*. **9**, 998–1011.
57. Gomes M. C., S. Silva M. A. F. Faustino, M. G. P. M. S. Neves, A. Almeida, J. A. S. Cavaleiro, J. P. C. Tomé and Â. Cunha (2013) Cationic galactoporphyrin photosensitisers against UV-B resistant bacteria: oxidation of lipids and proteins by 1O2. *Photochem. Photobiol. Sci*. **12**, 262–271.
58. Costa, L., C. M. B. Carvalho, M. A. F. Faustino, M. G. P. M. S. Neves, J. P. C. Tomé, A. C. Tomé, J. A. S. Cavaleiro, A. Cunha and A. Almeida (2010) Sewage bacteriophage inactivation by cationic porphyrins: influence of light parameters. *Photochem. Photobiol. Sci.* **9**, 1126–1133.
59. Merchat, M., G. Bertolini, P. Giacomini, A. Villanueva and G. Jori (1996) Meso-substituted cationic porphyrins as efficient photosensitizers of gram-positive and gram-negative bacteria. *J. Photochem. Photobiol.,* B. **32**, 153–157.
60. Lazzeri, D., M. Rovera, L. Pascual and E. N. Durantin (2004) Photodynamic Studies and Photoinactivation of Escherichia coli Using meso-Substituted Cationic Porphyrin Derivatives with Asymmetric Charge Distribution. *Photochem. Photobiol.* **80**, 286–293.

